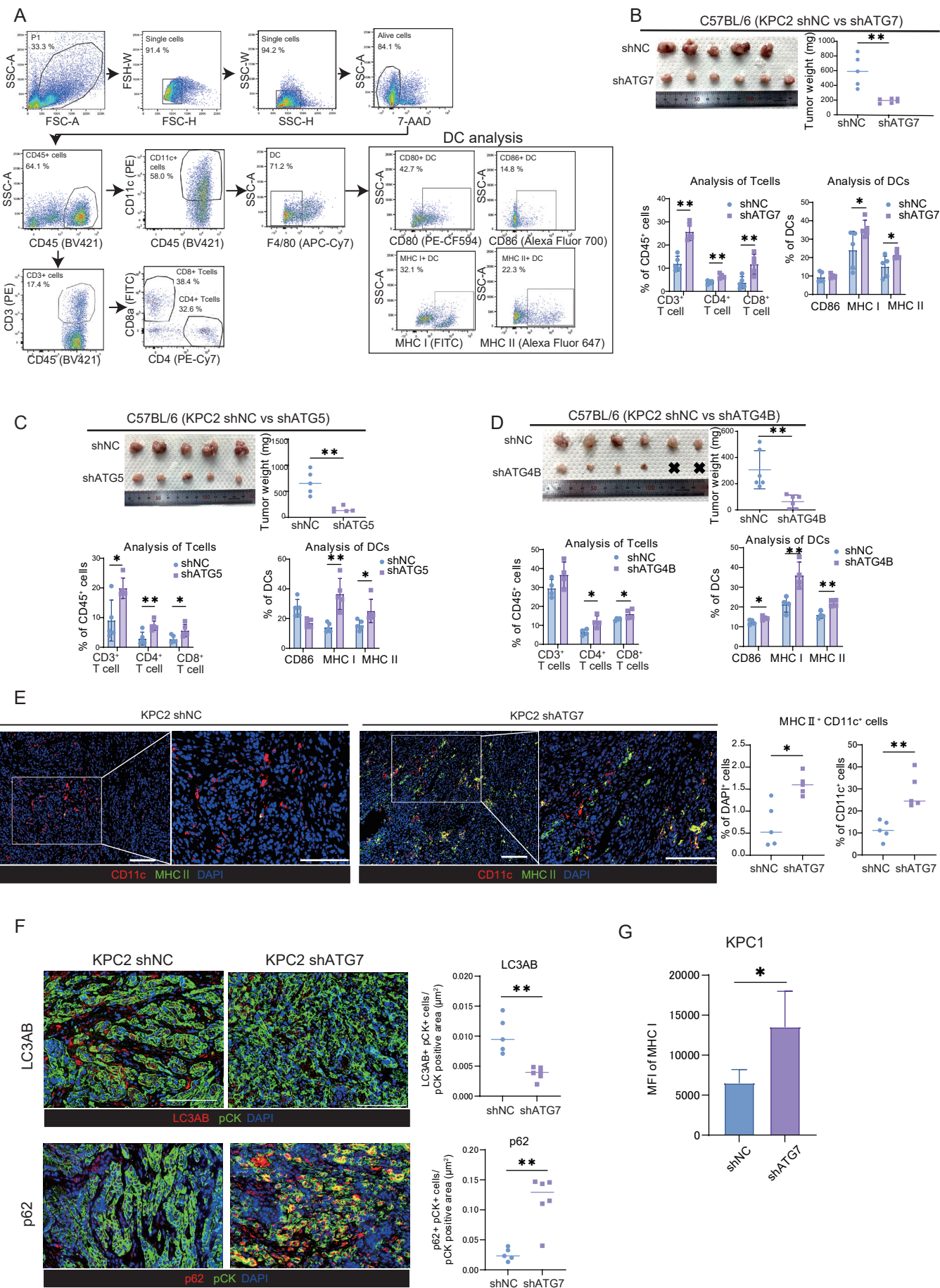


Supplementary Figure S4



Supplementary Fig. S4. Autophagy inhibition in cancer cells induces the activation of DCs in several murine autophagy-deficient PDAC models

(A) Flow cytometry gating strategy used in the analysis of murine tumors. Representative data is shown.

(B) KPC2 shNC or shATG7 tumors were orthotopically transplanted into C57BL/6 mice to compare tumor growth (upper). Tumor-infiltrating immune cell populations were analyzed using flow cytometry (lower).

(C) KPC2 shNC or shATG5 tumors were orthotopically transplanted into C57BL/6 mice to compare tumor growth (upper). Tumor-infiltrating immune cell populations were analyzed using flow cytometry (lower).

(D) KPC2 shNC or shATG4B tumors were orthotopically transplanted into C57BL/6 mice to compare tumor growth (upper). Tumor-infiltrating immune cell populations were analyzed using flow cytometry (lower).

(E) Results from an immunofluorescence analysis of orthotopic syngeneic KPC2 shNC/shATG7 tumors (Fig. S4B), showing activated DCs expressing CD11c (red) and MHC II (green). Representative images are shown. The graphs show the proportions of MHC II⁺ CD11c⁺ cells/DAPI⁺ cells (%) and MHC II⁺ CD11c⁺ cells/CD11c⁺ cells (%).

(F) Sequential IHC analyses were performed to evaluate the colocalization of LC3AB (red) / pCK (green), or p62 (red) / pCK (green). The graphs show the number of LC3AB⁺ pCK⁺ cells/pCK positive area and the number of p62⁺ pCK⁺ cells/pCK positive area.

(G) The expression of MHC I of CD45 negative cells derived from orthotopic syngeneic PDAC tumors (KPC1 shNC and KPC1 shATG7) were analyzed by flow cytometry.

Scale bars, 100 μ m (E). Bars, median; Error bars, mean \pm SD; * $p < 0.05$, ** $p < 0.01$, *** $p < 0.001$, **** $p < 0.0001$; ns, not significant; analyzed using the Student's t-test (B–G).